THE JOURNAL OF BIOLOGICAL CHEMISTRY
Vol. 271, No. 30, Issue of July 26, pp. 17911–17919, 1996

Printed in U.S.A.

The Organic Crystallizing Agent 2-Methyl-2,4-pentanediol Reduces DNA Curvature by Means of Structural Changes in A-tracts*

(Received for publication, March 20, 1996, and in revised form, May 15, 1996)

Mensur Dlakic‡, Kyusung Park§¶, Jack D. Griffith§, Stephen C. Harvey‖, and Rodney E. Harrington‡**

‡*From the Department of Biochemistry 330, University of Nevada at Reno, Reno, Nevada 89557, the* §*Lineberger Comprehensive Cancer Center, School of Medicine, University of North Carolina at Chapel Hill, Chapel Hill, North Carolina 27599, and the* ‖*Department of Biochemistry and Molecular Genetics, University of Alabama at Birmingham, Birmingham, Alabama 35294*

Contemporary predictive models for sequence-dependent DNA structure provide a good estimation of overall DNA curvature in most cases. However, the two current models differ fundamentally in their view of the origin of DNA curvature. An earlier model that associates DNA bending primarily, although not exclusively, with stretches of adenines (A-tracts) is based on results of comparative gel retardation, cyclization kinetics, hydroxyl radical cutting, and other solution measurements. It represents an intersection of wedge and junction models. More recently, a non-A-tract bending model has been proposed, built on structural results from x-ray crystallography and molecular modeling. In this view, A-tracts are proposed to be straight and rigid, whereas mixed sequence DNA is bent. Because a key premise of the non-A-tract bending model is the crystallographic observation that A-tracts are straight, we have examined the effect in solution of 2-methyl-2,4-pentanediol (MPD), an organic solvent used in crystal preparation for crystallographic DNA structure determinations. Using cyclization analysis, DNase I cutting, chemical probing, and electron microscopy on DNA oligomers with and without A-tracts, we show that the presence of MPD in solution dramatically affects A-tracts and that the effect is specific to these sequence elements. Combined with the previous observation that MPD affects gel mobility of curved sequences with A-tracts, our findings support the bent A-tract model and call for caution in the interpretation of crystallographic results on DNA structure as these are presently obtained.

Although the origin of DNA curvature has been extensively investigated over the past decade and a half, it remains elusive and highly controversial. Early attempts to rationalize DNA curvature were based upon the observation that short runs of helically phased adenine tracts (A-tracts) are necessary and sufficient to produce experimental results consistent with macroscopic DNA curvature. Thus, it was proposed that DNA bending is an intrinsic attribute of only certain DNA sequences, primarily AA·TT dinucleotide elements (1) or A_nT_m-tracts ($n + m = 3–6$) (2–6), and that *macroscopic* DNA curvature arises from additive, coherent contributions of these sequences phased with helical periodicity along the DNA. Two models were then proposed to explain the observed DNA curvature which differ primarily in the basic unit of DNA that is assumed responsible for the bending. The wedge model defines bending as a result of axial deflections (wedges) of successive AA·TT dinucleotides, whose vectorial sum describes the global DNA trajectory (1, 6–8). The junction model proposes that the bending arises from structural discontinuities at the junction of A-tracts, assumed to be in a modified B-DNA structure, with the adjacent B-form DNA (3, 9–11). At first, contributions of other DNA sequence elements were considered small and hence were ignored. More recently, however, evidence has accumulated suggesting that DNA curvature may involve additional sequence elements (12–15), and more sophisticated models were proposed which included all 16 wedge angles (16, 17). The wedge and junction models have both undergone refinement over the past decade (reviewed in Refs. 18–20) and have now largely converged into a single unifying view of DNA bending in terms of both magnitude and direction (summarized in Ref. 21).

The second principal model for DNA curvature maintains that A-tracts are straight and unwrithed, and provide requisite phasing relationships for general sequence B-DNA in which writhing is caused by positive roll angles. This bent non-A-tract model is based on early crystallographic and modeling studies of oligonucleotides containing A-tracts (22–26) and has been developed largely on the basis of more recent crystallographic structural studies (27–29). In the two models, a reverse symmetry in bending exists between A-tracts and general sequence DNA segments (28). According to the bent A-tract model, the bend is at the center of the A-tract and compresses the minor groove, while the bent non-A-tract model requires major groove-directed bending in the general sequence DNA regions. A compromise model, where the bent A-tract and bent non-A-tract models meet halfway, is one in which both A-tract and general sequence DNA bends are similar in magnitude and directed into the minor and major groove, respectively (21, 30).

It has been argued by proponents of both models that solution measurements alone cannot distinguish between the two because they measure only global curvature, from which local bending parameters must be deduced by simulations and computational analysis (18, 21, 28, 29). It seems clear that, with appropriate scaling of parameters and structural assumptions, both models can rationalize solution measurements quite well and, in most cases, can predict identical global DNA curvature despite distinctly different starting parameters (24, 28, 29, 31).

* This work was supported by National Science Foundation Research Grant MCB 9117488 (to R. E. H.), National Institutes of Health Grants HG00656 and CA70274 (to R. E. H.), GM31819 (to J. D. G.), and GM34015 (to S. C. H.), and by United States Department of Agriculture Hatch Project NEV032D through the Nevada Agricultural Experiment Station (to R. E. H.). The costs of publication of this article were defrayed in part by the payment of page charges. This article must therefore be hereby marked "*advertisement*" in accordance with 18 U.S.C. Section 1734 solely to indicate this fact.

¶ Present address: Laboratory of Biochemistry at NCI, Bldg. 37, Rm. 4D19, Bethesda, MD 20892.

** To whom correspondence should be addressed. Tel.: 702-784-4112; Fax: 702-784-1419; E-mail: harring@med.unr.edu.

However, Bolshoy *et al.* (17) have demonstrated that computational methods based upon measurements of global curvature from gel methods utilizing a sufficient body of experimental data and a diverse enough sampling of different sequences do indeed converge upon a unique set of local bending parameters, *e.g.* the 16 dinucleotide wedges. Thus, the limitation of gel-based methods to determine global DNA curvature would appear to be primarily statistical rather than fundamental. Dickerson and co-workers have argued that, to substantiate one model over the other, it is necessary to start from well defined locally bent DNA structures, and from these obtain global DNA curvature by simple mathematical computation (27, 28). Relying on the unique ability of crystallography to determine local DNA bending, these workers have asserted that the crystallographic observation of straight poly(A) tracts and curved general sequence DNA strongly favors the bent non-A-tract model for the prediction of macroscopic DNA curvature. Although this model appears to have better predictive power than the other in certain cases (29), and despite the undisputed power of crystallography as a structural tool, this kind of analysis is unable to rationalize all available solution data (21, 31). It is also disturbing that some aspects of the bent non-A-tract model lack critical support from several structures of general B-DNA sequences solved thus far by x-ray crystallography (21, 31, 32). Finally, it has been shown recently that the presence of 2-methyl-2,4-pentanediol (MPD),[1] a reagent used in growing crystals, reduces the curvature in sequences with A-tracts (32), thus raising serious questions about the use of x-ray crystallography to determine origins of local bending under such conditions.

In the present work, we have performed a series of experiments designed to test the effects of MPD on local bending in poly(A) tracts. Such effects might account for the differences observed between crystallographic and gel mobility experiments in solution with attendant implications for the general applicability of the bent non-A-tract and bent A-tract models. We report here the results of T4 ligase-mediated cyclization, DNase I cutting, chemical probing, and electron microscopy (EM). In addition to curved DNA sequences containing A-tracts, we have examined curved DNA sequences without A-tracts as controls (15, 30, 33) and combinations of both types of sequence. Our results clearly demonstrate that poly(A) tracts in the absence of MPD exhibit fixed curvature, but that MPD concentrations significantly lower than those typically used in crystal growing effectively straighten these bends either through reduction in fixed curvature or through enhanced flexibility. In addition, a comparison of the various experimental results unambiguously demonstrates that the MPD effect is directed specifically to A-tracts under the experimental conditions used in our studies. These results suggest that additional crystallographic experiments on poly(A)-containing oligonucleotides in the absence of MPD or other dehydrating reagents, and with proper controls for crystal packing effects, are required before any DNA curvature model based upon crystallographic results can be accepted.

MATERIALS AND METHODS

DNA End Labeling and Ligation—Oligonucleotides were purified on 20% denaturing polyacrylamide gels. Macerated gel slices were soaked overnight in a buffer containing 0.5 M ammonium acetate and 1 mM EDTA, followed by desalting of the eluate on Sephadex columns. T4 polynucleotide kinase was used to label 5′ ends with [γ-^{32}P]ATP (50 μCi). Complementary strands were mixed, heated to 90 °C, and brought gradually to room temperature. After annealing, samples were run on a 5% native polyacrylamide gel to separate duplex from labeled single-stranded DNA. Following elution and desalting, DNA duplexes were self-ligated in the ligase buffer using 400 units of T4 DNA ligase. MPD was added where indicated to a concentration of 10–20% (v/v). The reaction in 20% MPD was slowed down due to greatly reduced T4 ligase activity, so we based our interpretation on experiments with 10% MPD, where the enzyme activity was normal. Ligation proceeded overnight on ice.

Gel Electrophoresis—Products of the overnight ligation were analyzed by two-dimensional polyacrylamide gel electrophoresis (30, 34). The first dimension was 5% polyacrylamide (19:1 ratio of mono:bisacrylamide) containing 25% glycerol. Electrophoresis was stopped when a xylene cyanole dye marker migrated 9.5 cm on a 14-cm long gel. The lane containing ligation products was excised and placed horizontally between slab gel plates. An 8% second dimension gel containing 10% glycerol and 50 μg/ml chloroquine phosphate was then polymerized around it. Separated DNA species were located with autoradiography on wet gels, and representative spots were excised from the gel for size determination. Excised spots containing both linear and circular DNA fragments were macerated and eluted overnight, the DNA was denatured, and fragment sizes were determined by comparative electrophoresis on 8% denaturing polyacrylamide gels against the original ligation products.

DNase I Cutting—For DNase cutting reactions, DNA samples were prepared as above for ligation except that only one strand was end labeled. DNase I cutting was done for 1 min in a buffer containing 100 mM Tris-HCl and 10 mM $MgCl_2$ (pH 7.6), using 0.001 unit/ml enzyme. MPD was added to a final concentration of 20% (v/v). The reaction was stopped by adding EDTA to 5 mM, and by phenol-chloroform extraction. Products of cutting were separated on a 15% gel, and autoradiographs were scanned using an UltroScan densitometer and GelScan XL software (Pharmacia Biotech Inc.). Each peak from the gel was assigned a numerical value and corrected for multiple cuts between bond *n* and the radioactive label (35, 36). Cleavage probabilities (relative cutting frequencies) were then calculated as natural logarithms of corrected values. For samples containing MPD, linear regression was used to scale cleavage probabilities down to levels comparable to those in its absence.

Hydroxyl Radical Cutting and Chemical Probing—Hydroxyl radical ('OH) cutting in the absence of MPD was performed as described previosuly (37), with quantities of the various components adjusted to a total volume of 50 μl. Only the 5′ end of one strand was labeled. In samples containing MPD, concentrations were 15% (v/v). Since MPD quenches 'OH, the hydrogen peroxide concentration was increased three times to a final concentration of 0.09%. Potassium permanganate and diethyl pyrocarbonate (DEPC) cutting procedures followed McCarthy *et al.* (38), and the final reaction volume was 50 μl. Where indicated, 20% MPD (v/v) and 10 mM $MgCl_2$ were added before cutting to evaluate their individual and combined effects on DNA structure. Products of the cutting reactions were separated on 20% denaturing polyacrylamide gels, and densitometric analyses were done from scanned images using NIH Image 1.59 software.

Electron Microscopy—A 219-bp fragment of kinetoplast DNA from *Crithidia fasciculata* was examined by EM. This was one of the first naturally occurring curved DNAs to be investigated (39), and it has previously been characterized by EM (40). The sequence of the 225-bp precursor (41) is shown in Fig. 1*b*. This precursor was cloned into pGEM3Zf(+) at the *Bam*HI site (pYW9). The plasmid was digested with *Bam*HI at the *underlined* GG steps, giving the final 219-bp fragment. The restriction enzyme was removed by phenol extraction, and the DNA was precipitated with ethanol. The DNA precipitate was dissolved in a buffer of 10 mM Tris, 0.1 mM EDTA (pH 7.5) and diluted with a mixture of this buffer and the appropriate MPD concentration to give a final DNA concentration of 1 μg/ml. Samples were prepared with MPD concentrations ranging from 0 to 50%, in 10% increments.

The preparation of the samples for EM followed Griffith and Christiansen (42). After incubation at room temperature for at least 10 min, the DNA solution was applied to a freshly glow-charged thin carbon foil supported by a copper grid, using a buffer containing 2.5 mM spermidine. The samples were then washed with graded water-ethanol solutions and air-dried. The samples were rotary shadowcast with tungsten at 1×10^{-6} Torr (1 Torr = 133.322 Pa). At least 300 molecules were scored at each MPD concentration except at 40% MPD, where only about 100 molecules could be scored because of high background. Efforts to examine samples at 50% MPD were unsuccessful because backgrounds were too high to permit data collection.

DNA curvature analysis was carried out using software developed by R. Rubin in the laboratory of J. D. G. In brief, curvature was measured using a two-step procedure, data collection and data analysis. Data collection consisted of photographing DNA molecules at the EM and

[1] The abbreviations used are: MPD, 2-methyl-2,4-pentanediol; bp, base pair(s); 'OH, hydroxyl radical; DEPC, diethyl pyrocarbonate; EM, electron microscopy.

a

```
AGAGAAAAAGAGAGAAAAAAGAGAGAAAAAAG                    Atr
AGAGGGCCCGAGAGGGGCCCGAGAGGGGCCCG                    non-Atr
CCCAAAAAGGGCCAAAAAGGG                               21ga
CCCAAAAAGGGCCAAAAAGGGCCCAAAAAGGGCCAAAAAGGG          42ga
```

b

```
        GG ATCCCCTAAA ATTCCTTCCG AAAATCGCGA GGTTACTTTT
TTGGAGCCCG AAAACCACCC AAAATCAAGG AAAAATGGCC AAAAAATGCC
AAAAAATAGC GAAAATACCC CGAAAATTGG CAAAAATTAA CAAAAAATAG
CGAATTTCCC TGAATTTTAG GCGAAAAAAC CCCCGAAAAT GGCCAAAAAC
GCACTGAAAA TCAAAATCTG AACGTCTGGA TCC
```

FIG. 1. **All sequences are shown from the 5′ end.** *a*, sequences used for ligation and cutting studies. Complementary strands for *Atr* and *non-Atr* were designed to provide 3-bp long overhangs at 5′ ends, thus ensuring directional ligation. Those portions of each sequence that differ from the other are *underlined*. Complementary strands for *21ga* and *42ga* produced 3-bp long 3′ overhangs. *b*, initial 225-bp fragment with phased A-tracts used to obtain the 219-bp sequence for EM studies (see "Materials and Methods").

projecting the photographic images of the DNA onto a Summagraphics digitizing tablet. Each DNA molecule was then traced using the cursor of the digitizing tablet connected to a CompuAdd computer, which stored the raw data as a series of *x*, *y* coordinate points. End-to-end distances and contour lengths were calculated from the data using an in-house data analysis program.

Curvature is easily monitored by measuring the normalized end-to-end distance,

$$D = d_{ee}/d_{cl}, \qquad \text{(Eq. 1)}$$

which is the ratio between the end-to-end distance (d_{ee}) and the contour length of the molecule (d_{cl}). For highly curved molecules this ratio is small, and it approaches one for extended molecules.

RESULTS

DNA Cyclization—The basic idea of the experiment was to test the MPD effect on DNA sequences for which cyclization patterns in normal conditions were known from previous studies (43). Sequences used in this study are shown in Fig. 1*a*. Two-dimensional gel analysis of the A-tract-containing oligonucleotide (sequence *Atr* in Fig. 1*a*) showed that cyclization efficiency is dramatically reduced in the presence of MPD (Fig. 2*A*). In the same assay conducted in the absence of MPD, this sequence cyclizes into microcircles as small as 160 bp (43). In the control sequence, the A-tract was replaced with the GGGCCC motif (*non-Atr* in Fig. 1*a*). Bending in this motif is of similar magnitude but opposite in direction from A-tract bending (15, 30, 33). Similar bending has been reported in its subset sequence, GGCC (27, 44). Sequence non-Atr was designed with two principal objectives: (i) to keep it as unchanged from Atr as possible (both sequences share an identical GAGAG motif); and (ii) to retain similar global curvature and cyclization properties as Atr. The latter objective is clearly upheld, as demonstrated in an independent analysis (43). The non-Atr control sequence produces circles as small as 160 bp both in the presence and absence of MPD, and the cyclization patterns are virtually identical in the two cases (Fig. 2*B*) (43). Clearly, cyclization in the presence of MDP is affected by this reagent only for the A-tract-containing oligonucleotide.

To further explore the specificity of the MPD effect, the A-tract and GGGCCC motif were joined together into a single sequence with appropriate phasing relationships to obtain maximal curvature (*21ga* in Fig. 1*a*). This sequence formed extremely tight microcircles of 105 bp (Fig. 3*A*), as expected when two motifs which bend in opposite directions and assume

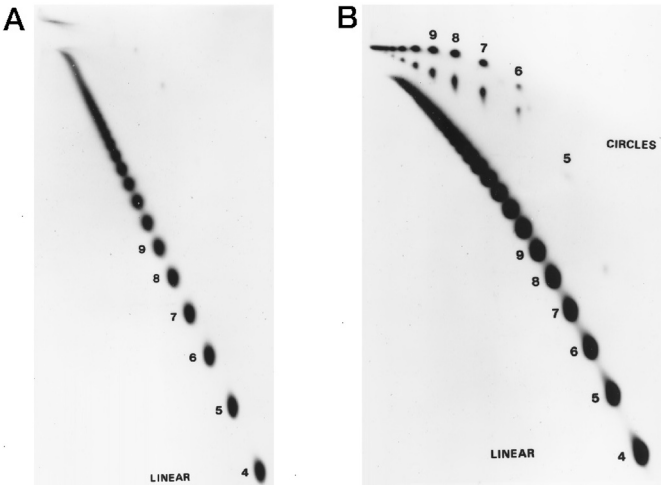

FIG. 2. *A*, second dimension of the two-dimensional polyacrylamide assay of sequence Atr and *B*, of sequence non-Atr. In both cases, 10% MPD was added to the ligation mixture. The first dimension was run left to right with respect to the orientation of the figure, and the second dimension from top to bottom. Circles and linear fragments are denoted by a value corresponding to the number of ligated oligomers.

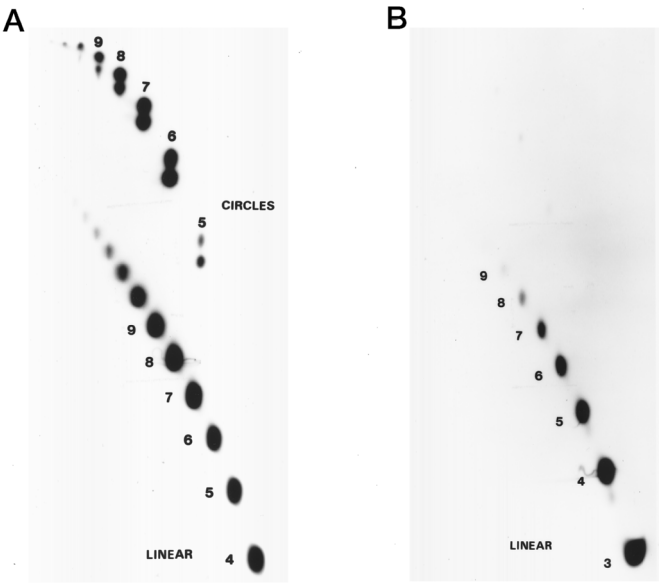

FIG. 3. *A*, two-dimensional polyacrylamide assay for 21ga shows strong circle formation starting at 105 bp (5 starting oligomers). *B*, the same sequence ligated in the presence of 10% MPD has a dramatically reduced yield of circles.

inverse rotational positions in nucleosomes are placed half a helical turn apart (12, 30, 45, 46). On the other hand, the efficiency of cyclization dropped dramatically upon the addition of MPD to the ligation buffer (Fig. 3*B*). We showed above that curvature in the GGGCCC motif appears insensitive to MPD in contrast with the effects of this reagent on A-tract curvature (compare non-Atr *versus* Atr in Fig. 2). Although the above experiments clearly show that MPD reduces A-tract curvature but does not affect the GGGCCC motif, the reduction of curvature in 21ga seems greater then the sum of these two results, thus indicating synergistic effects of MPD in this case.

DNase I Cutting—To obtain more detailed information on conformational changes induced by MPD, we used DNase I to probe the DNA structure of all the oligonucleotides listed in Fig. 1*a*. In all cases, enzymatic cleavage was markedly higher when MPD was added to the digestion buffer. Furthermore, all regions in the sequences exhibited increased susceptibility to DNase I attack. Fig. 4 shows a schematic representation of

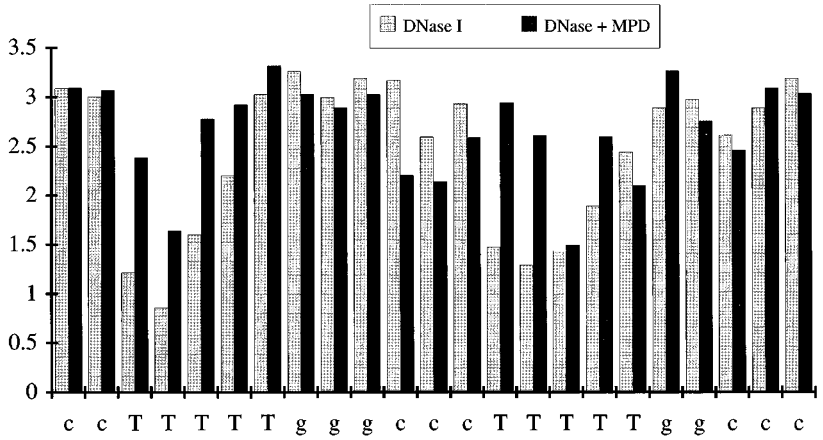

FIG. 4. **Probabilities of cleavage (ln *p*) for the complementary strand of 42ga obtained by DNase I.** *Light bars* represent cutting with DNase I in ordinary conditions. *Dark bars* denote DNase I cutting with 20% MPD in the reaction buffer. Since cutting frequencies in the latter case were much higher, they were uniformly scaled down by factor 4.17 to make them comparable to DNase I cutting without MPD. They were afterward corrected for multiple cuts and expressed as natural logarithms (35, 36). Nucleotide sequence on the *x* axis is shown from the 5′ end.

DNase I cutting frequencies for the sequence *42ga*, both in the presence and in the absence of MPD. Those obtained with MPD present (*dark bars*) were scaled down for the sake of comparison (see "Materials and Methods"). Although the cleavage probabilities for all nucleotides were considerably increased in the presence of MPD, the relative cutting increase is most prominent within A-tracts, suggesting that the flexibility and/or minor groove geometry have changed most dramatically in this sequence motif (36, 47–49).

Hydroxyl Radical Cutting and Chemical Probing—All sequences from Fig. 1*a* except 21ga were examined using ·OH, $KMnO_4$, and DEPC chemical probes. Cutting profiles by ·OH and $KMnO_4$ are shown in Fig. 5. Because of its higher reactivity toward thymines (50, 51), $KMnO_4$ was used preferentially to probe the structure of A-tracts in their complementary strands (Fig. 5, *right-hand side*). In similar fashion, DEPC was used to probe the DNA strands containing adenine runs, since it preferentially cuts these nucleotides (data not shown).

Although hydroxyl radicals cleave DNA with little sequence specificity, they have nevertheless provided valuable insights into sequence-dependent DNA structure (52, 53). They produce a highly specific cutting pattern within A-tracts characterized by a steady decrease in reactivity from the 5′ to 3′ end, which is generally interpreted as a smooth decrease in its minor groove width, since the minor groove provides the principal access of the radicals to their cleavage site (54). We have observed this same cutting pattern in our sequences containing A-tracts (*top portions* of Fig. 6, *a* and *b*). However, upon addition of MPD, this characteristic pattern disappears completely in sequence Atr (Fig. 6*b*, *bottom*), and becomes reversed in 42ga (Fig. 6*a*, *middle*). In the presence of MPD, ·OH cleavage patterns in A-tracts become indistinguishable from those observed in general-sequence DNA. The only notable differences in ·OH cutting outside A-tracts are observed in adenines within the GAGAG motif (Fig. 6*B*). It is interesting that Mg^{2+} in conjunction with MPD returns ·OH cutting back to normal levels in one A-tract (outside the boxed region in Fig. 6*A*, *bottom part*), while the cutting of the other A-tract remains similar to general-sequence DNA (inside the boxed regions in Fig. 6*A*, *bottom part*). There were no significant differences in ·OH cutting with only Mg^{2+} added compared to the reaction in an ordinary cutting buffer (data not shown).

Cutting with potassium permanganate also demonstrates that MPD-induced structural changes are primarily localized within the A-tract (Fig. 7, *top* and *middle portions*). Again, these changes are partially nullified when Mg^{2+} was added along with MPD (Fig. 7, *bottom part*). Neither ·OH, $KMnO_4$, nor DEPC probes detected significant MPD-induced structural changes in any part of the non-Atr sequence (data not shown).

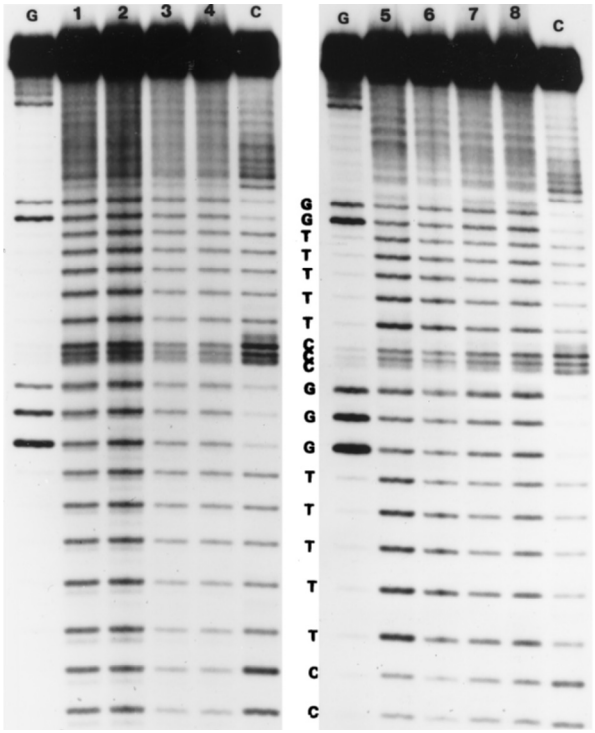

FIG. 5. **Hydroxyl radical and $KMnO_4$ cutting of the complementary strand of 42ga.** *Lanes G* and *C* correspond to guanine- and cytosine-specific reactions, respectively. *Lanes 1–4* contain ·OH cutting products: *1*, with 10 mM $MgCl_2$ in the reaction buffer; *2*, in TE buffer (10 mM Tris, 1 mM EDTA, pH 7.5); *3*, with 15% MPD added; *4*, with both 10 mM $MgCl_2$ and 15% MPD added. *Lanes 5–8* correspond to *lanes 1–4*, except that cutting was done by $KMnO_4$. The sequence ladder in the *middle* (shown incomplete for clarity) applies to both sides of the figure. It also corresponds to the densitometric profile in Fig. 7.

Electron Microscopy—Fig. 8, *a–e*, presents the distributions for the normalized end-to-end distance (*D*) of the kinetoplast fragment at different concentrations of MPD. In the absence of the dehydrating agent, the curvature of this fragment is reflected by both the low mean (0.28) and median (0.16) values for *D*. As the MPD concentration is raised, both of these quantities increase monotonically, slowly at first, then more rapidly beyond an MPD concentration of 20% (Fig. 8*f*). This reflects the

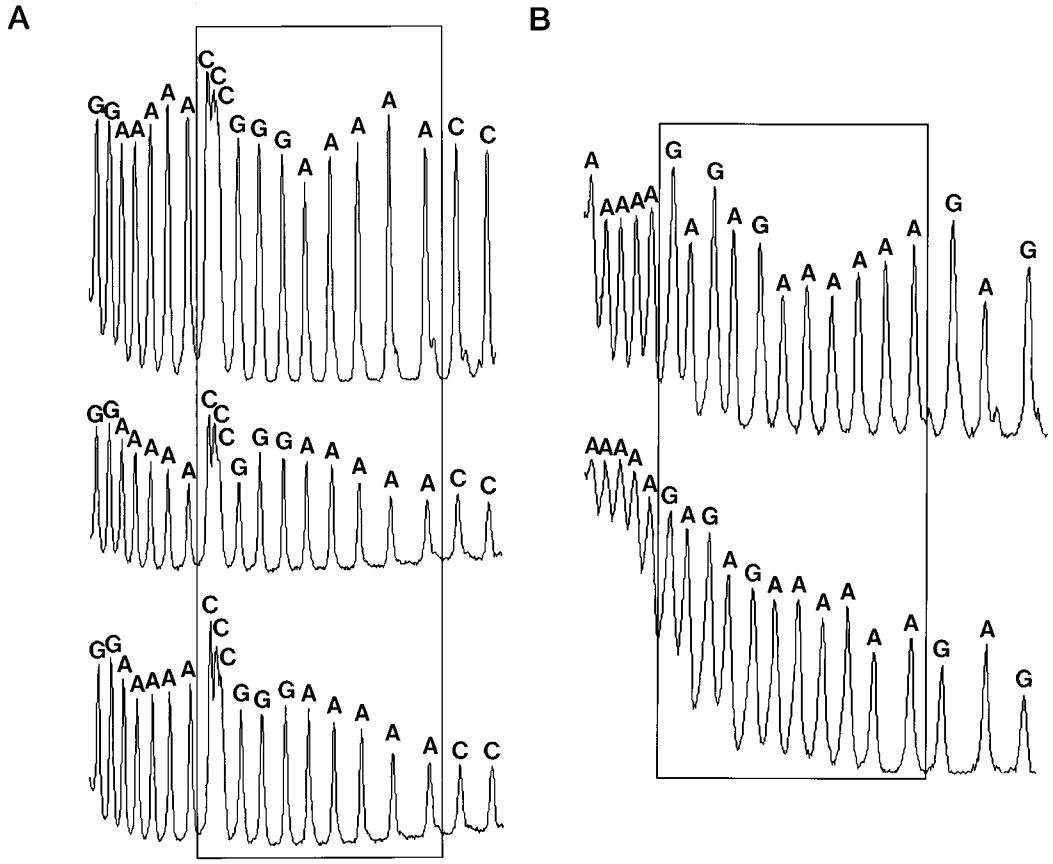

FIG. 6. *A*, densitometric profiles for 42ga cut with ·OH: in TE buffer (*top*), in 15% MPD (*middle*), and with both 10 mM $MgCl_2$ and 15% MPD (*bottom*). Relatively lower cutting frequencies in the latter two profiles are the result of partial quenching of ·OH by MPD. *B*, densitometric profiles of Atr cut with ·OH: in TE buffer (*top*) and with 15% MPD added (*bottom*). In both cases the basic repeat within the sequence is *boxed*. The *left-hand side* corresponds to the 3′ end of the strand.

simultaneous reduction in the fraction of highly curved molecules (small values of *D*) and the increase in the fraction of extended molecules (high values of *D*). Clearly, MPD reduces the curvature in the kinetoplast fragment. This is consistent with earlier studies on the anomalous mobility of this fragment in polyacrylamide gels. This anomaly is one of the hallmarks of DNA curvature, and it is monotonically reduced as the MPD concentration increases (32).

DISCUSSION

T4 ligase-mediated DNA cyclization has been widely used to study DNA structure (30, 55–57), and it has provided a quantitative evaluation of A-tract bending (7, 34, 58). Cyclization kinetics measurements can provide true cyclization probabilities (56), and conditions can generally be found for which the results of mixed ligation cyclization experiments can be interpreted semiquantitatively (34, 59). Thus, cyclization experiments complement gel migration studies and offer a desirable alternative in those instances where results from the latter are inconclusive. A secondary advantage of cyclization studies is that ligase enzymes require typical physiological levels of Mg^{2+}, and the presence of divalent ions seems essential for a general view of DNA curvature (30, 33).

We have used this approach to study the effect of MPD on DNA sequences in oligonucleotides of known cyclization properties. Comparative analysis between Atr and non-Atr was the first indication that MPD specifically targets A-tracts (Fig. 2). This was further confirmed when GGGCCC motifs and A-tracts were tandemly joined into a single sequence. Despite the insensitivity of the GGGCCC motif to MPD in non-Atr (Fig. 2*B*), this motif was not able to cyclize efficiently in MPD when joined by an A-tract. The contributions of A-tracts to the DNA bending can be also inferred from Fig. 3*A* alone. The smallest circles (105 bp) contain 10 GGGCCC motifs and 10 A-tracts. If A-tracts are assumed straight, each GGGCCC motif would have to bend by 36° in order to produce circles that small. This number is ~50% larger than the recent estimate of GGGCCC bending by cyclization (30) or the 23° obtained by x-ray crystallography using a similar sequence motif (27). DNA flexibility can account for part of the bending observed in cyclization experiments (56, 60, 61). However, since the length of the cyclizing molecules (105 bp) is well below the persistence length of random sequence DNA (~150 bp), its flexibility must be relatively small (60). Thus, *at least* the difference between 20–24° and 36° must come from A-tracts. This result seems clearly to require that the A-tracts and GGGCCC motifs both bend, but in opposite directions, as proposed earlier (15, 30).

Possible effects of MPD on T4 ligase activity, and thus indirectly on cyclization kinetics, are ruled out in Fig. 2, where strong activity of the enzyme is confirmed by very large linear ligation products in the lower diagonal. The enzyme activity was found to be normal by these criteria over the concentration range of 10–15% (see "Materials and Methods"), although it was somewhat diminished in 20% and higher MPD concentrations (data not shown). The fact that circles were weakly formed even in 10% MPD (Figs. 2*A* and 3*B*) indicates that some bending may occur at the lowest MPD concentrations studied and that the DNA is not fully straightened until the higher MPD concentrations typically used in crystallographic studies are attained. An increase in the MPD effect is especially apparent in the EM experiments (see below) and resembles the

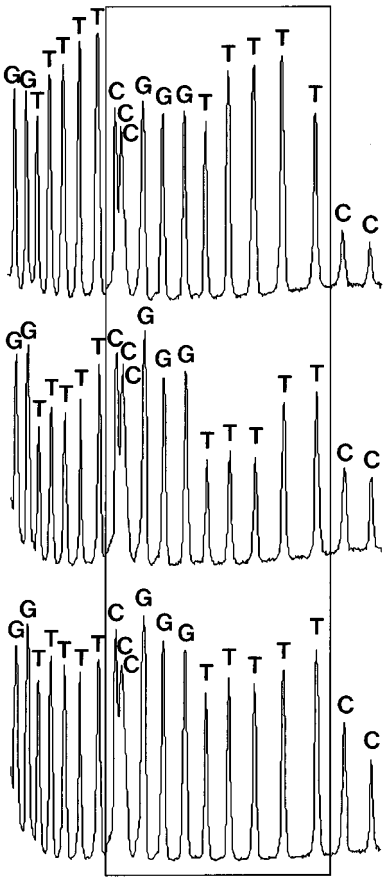

FIG. 7. **Densitometric profiles for the lower strand of 42ga cut with $KMnO_4$: in TE buffer (*top*), in 20% MPD (*middle*), and with both 10 mM $MgCl_2$ and 20% MPD (*bottom*).** The basic repeat within the sequence is *boxed* and the *left-hand side* corresponds to the 3′ end of the strand.

gradual decrease in the DNA gel mobility anomaly with a step-by-step increase in temperature noted by other investigators (10, 62, 63). Cyclization efficiency can also be altered by changes in overall helical twist (56, 57, 64), so if the addition of MPD changes the helical repeat in the sequences studied, the proper end alignment required for efficient head-to-tail ligation might be reduced. However, Sprous *et al.* (32) showed, using topological assays, that MPD has no effect on the helical repeat of DNA.

DNase I is one of the rare endonucleases with considerable sequence specificity in cutting, reflecting local variations in minor groove dimensions and in bendability toward the major groove (35, 36, 47, 49, 65, 66). It has therefore been widely used as a molecular probe for DNA structure (12, 35, 49, 67, 68). In the DNase I cutting experiments reported here, in the presence of MPD, the greatest increase in cutting efficiency is observed for A-tracts, although all sequence elements are so affected to some degree (Fig. 4). It should be noted that cleavage probabilities in the presence of MPD are fairly uniform, but the proportionally higher cutting of A-tracts is a result of the initially weak cutting within this region. A similar trend in DNase I cutting of A-tracts was observed in early experiments with another dehydrating agent, dimethyl sulfoxide (35), and also when cleavage was done at increased temperatures (35, 69). In addition, dimethyl sulfoxide changes CD and absorbance spectra of poly(dA)·poly(dT) in a manner similar to temperature (69). These observations suggest that dehydrating agents and increased temperature lead to similar changes in hydration patterns around DNA, particularly in A-tracts, which translate into the widening of the minor groove and/or increased flexibility sensed by DNase I. Such static and dynamic structural changes affect the time-averaged properties of A-tracts, which are otherwise characterized by a very stable curvature under normal conditions (30), and explain their reduced mobility anomaly in gels containing ethanol and MPD (32, 62). DNase I cutting in solution and in the presence of Mg^{2+} has shown remarkably good predictive power, implicating DNA structure in many DNA-protein complexes (49), and should have even greater promise once contributions to the cutting frequency from static and dynamic structural effects are separated.

Chemical probes have been widely used in recent years as powerful tools to identify unusual local structures in DNA (70). When carefully employed, their chemical action can usually be determined at single nucleotide resolution. In the present work, they provide direct evidence that structural changes induced by MPD are located in A-tracts. This is especially clear in the modification of the characteristic ·OH cutting profile observed in Fig. 6. It reflects changes in minor groove width similar to those obtained with sequence motifs that disrupt the unique A-tract structure (71, 72). These studies also show that the presence of Mg^{2+} leads to a partial reversal or neutralization of the MPD effect in A-tracts. This cannot be a complete reversal, however, since the enzymatic experiments, *i.e.* DNase I and cyclization, are performed in the presence of Mg^{2+} and yet their results are consistent with the other experiments described here. The dehydrating effect of Mg^{2+} binding is lowest for the most hydrated DNA sequences, namely for regions rich in A·T base pairs (73). A similar effect was observed in gel mobility experiments on sequences with and without A-tracts (33, 43). However, once the hydration of A-tracts is disrupted upon the addition of MPD, it is possible that binding of Mg^{2+} changes for these regions. It is not yet clear whether MPD and Mg^{2+} function synergistically or whether they interact with the DNA in a mutually exclusive fashion.

The EM results demonstrate clearly that MPD reduces DNA curvature in a DNA sequence containing phased poly(A) tracts. In control experiments without MPD, the kinetoplast DNA fragment investigated exhibits a very small values of *D*, the ratio of end-to-end distance to contour length (Fig. 8*a*), indicating that the DNA molecules are nearly circular in shape as a result of strong macroscopic curvature. A similar conclusion was reached in earlier studies of a comparable fragment (40). As the MPD concentration is increased, the distribution is shifted toward larger values of *D* (Fig. 8*e*). Mean and median values of *D* show a systematic increase with increasing MPD concentrations (Fig. 8*f*), suggesting that the MPD effect may depend upon the extent of DNA dehydration by this reagent. The relatively smaller increase in *D* up to a MPD concentration of ~20% is consistent with the fact that some circles were still observed in cyclization experiments at 10% MPD (Figs. 2*A* and 3*B*), and indicates that DNA curvature is not completely abrogated until higher MPD concentrations are used. Because 30% or higher MPD has been used in the crystallizing of all A-tract sequences solved thus far by crystallography (74), it is likely that MPD effects in these studies are more pronounced even than in our experiments. The EM results complement gel mobility experiments on the same DNA fragment, where the retardation anomaly, as a criterion of DNA curvature, steadily decreases with increased concentrations of MPD (32). In an analogous way to the similar temperature and MPD effects discussed above for DNase I cutting, an increase in temperature has been shown to produce similar changes in kinetoplast DNA curvature as the present observations with increasing MPD (62, 75).

Dickerson and colleagues (74) have recently argued that MPD does not significantly affect DNA bending in crystals.

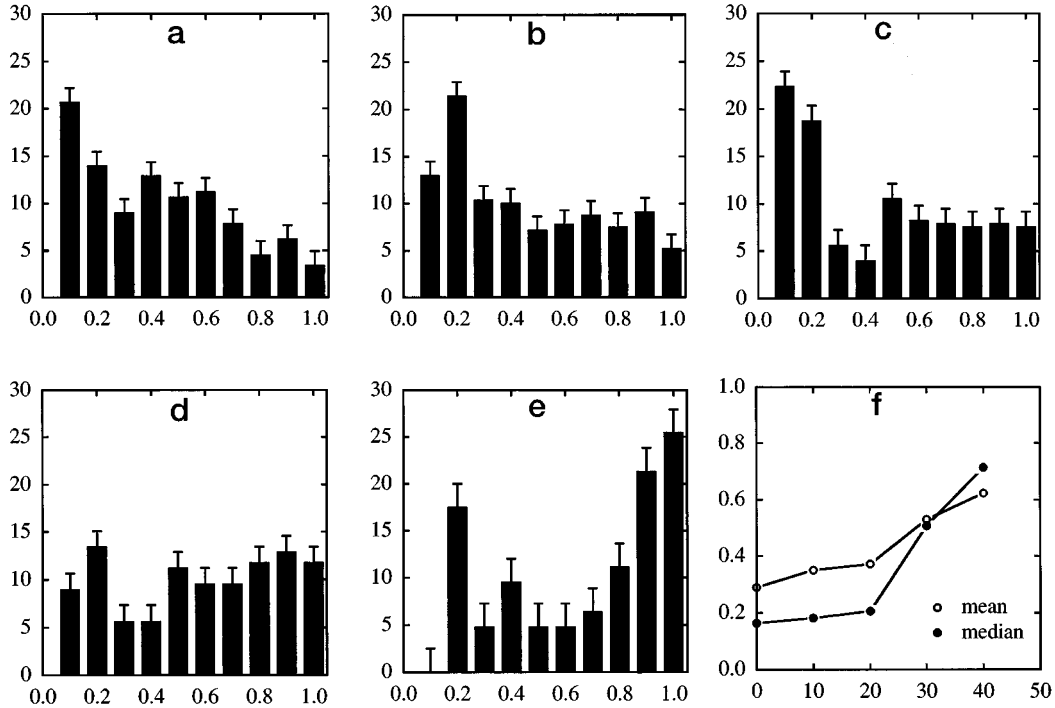

FIG. 8. *a–e*, probability distribution of normalized end-to-end distances (*D*) for a 219-bp fragment (Fig. 1*b*) as determined by EM studies. Each histogram represents the percent of molecules falling into the specified range of D at MPD concentrations of: *a*, 0%; *b*, 10%; *c*, 20%; *d*, 30%; *e*, 40%; *f*, mean and median values of normalized end-to-end distance (D_{ee}/D_{cl}) of a 219-bp DNA fragment as a function of MPD concentration. The steady increase in D_{ee}/D_{cl} with rising MPD concentrations is an indication of reduced DNA curvature (*i.e.* the molecules become more extended).

While the issue of MPD effects on DNA *in crystals* must be clarified by additional crystallographic experiments in the absence of MPD, very diverse experimental approaches described above show that MPD has a very profound effect on DNA structure *in solution*, even at much smaller concentrations then those typically used for the growth of DNA crystals. In addition, our results also suggest that MPD effects are directed specifically to A-tracts, thus offering a plausible explanation why bends within A-tracts have not been seen in crystals (74). Assuming that the effects of temperature and MPD are similar, our results obtained with DNase I support the suggestion that temperature changes the flexibility of A-tracts, and to a lesser extent the flexibility of general sequence DNA. This in turn may explain the rich variety of general sequence bends observed in DNA crystals (74) through increased bendability of these sequences facilitated by MPD. However, the hydroxyl radical cutting and chemical probing results, which are sensitive primarily to static structural features of DNA, suggest that MPD-induced variations translate into static changes in DNA structure only in the case of A-tracts, and that they are far more complex than might be inferred from the increased DNA flexibility of A-tracts alone.

CONCLUSIONS

Regions in B-DNA with a narrow minor groove, especially those rich in A and T, contain a hydration spine that sets them apart from other DNA sequences (76–81). The significantly more hydrated state of A·T base pairs, as compared to G·C and d(AT)·(AT), has been demonstrated by ultrasonic velocity measurements (82, 83), and by volumetric and calorimetric changes upon netropsin binding to DNA (84). Several excellent physical and thermodynamic studies (69, 75, 85, 86) have also linked hydration changes in poly(dA)·poly(dT) and A-tracts, but not in general-sequence DNA, with a temperature-induced loss of DNA curvature (10, 63). Furthermore, these studies demonstrate that the effects of a number of dehydrating agents on A-tracts are similar and parallel our results with MPD. Since both temperature and organic solvents evidently dehydrate DNA and affect A-tracts particularly, it is not likely that the structure of A-tracts obtained under stringent dehydrating conditions will be the same as in solution. It is likely that changes in hydration alter structural and dynamic features of A-tracts such as minor groove width and bendability toward the major groove, either independently or together. At high concentration, MPD alters the dielectric constant of the medium and might exert effects through other mechanisms in addition to dehydration. This question will require additional study.

Structural changes in A-tracts due to the presence of MPD are explainable in two ways, depending upon which bending model is chosen as a starting point. In terms of the bent A-tract model, our results require that A-tracts are straightened by MPD from a curved conformation in its absence. In other words, the presence of MPD induces more positive roll angles within A-tracts, which leads to the observed reversal of the gel mobility anomaly (32), reduced efficiency of cyclization, general sequence-like cutting with ·OH, and an increased ratio of end-to-end distance over contour length of DNA as seen in direct imaging by EM. This can also explain why A-tracts are straight in crystallographic studies, since equivalent or greater concentrations of MPD than used in the present work are employed in the crystal growing process. On the other hand, the bent non-A-tract model is generally compatible with our results although this requires certain rather extreme assumptions that have not been substantiated experimentally (21, 30, 31). If it is assumed that A-tracts are normally straight, but that positive roll angles are induced upon the addition of MPD, the resulting helical deflection within A-tracts would partially or completely cancel contributions of bent sequence motifs in B-DNA positioned half a helical turn away. Our results do not permit an unambiguous choice between these possibilities. Nevertheless, if it is assumed that the effects of MPD are similar in crystals and in solution under the conditions of our experiments, the fact that A-tracts are observed to be straight in crystals grown

with MPD necessarily supports the bent A-tract model. This view is also supported by additional independent observations (30, 43), and discussed at length elsewhere (31, 32).

The results presented here make it clear that no currently available predictive model for sequence-dependent DNA structure is fully complete and entirely unambiguous, and much additional work remains to be done before this goal can be achieved. Gel mobility experiments have provided important information on both global and local DNA curvature. They have uncovered only a limited number of sequence motifs that contribute strongly to overall DNA curvature, namely poly(A) tracts and GGGCCC motifs in the presence of Mg^{2+} (33), although mathematical analysis of gel mobility experiments shows that virtually all of the 16 dinucleotide sequence elements can make weaker contributions (17). However, current structural models developed from gel-based experiments neglect sequence-specific flexibility (87) and cannot account for recently reported effects of Mg^{2+} ion (33, 43) and sequence-context effects (43) (see also Ref. 19). This situation will undoubtedly improve in the future with additional experimental and theoretical/computational investigations (87–89). Crystallographic studies, in principle, provide unique information on details of sequence-dependent DNA structure at atomic levels of resolution, but the results reported here cast serious doubt on their general validity and therefore on the applicability of structural models derived from them. All crystallographic studies to date show straight poly(A) tracts (22, 23, 26), but bending is observed in several other sequence motifs (27, 28, 44). The present results do not challenge these latter results nor do they imply any specific MPD effect in their acquiring, since we find that MPD evidently does not affect the curvature of general sequence DNA. However, crystallographic and gel-based experimental results on DNA structures, which are in principle highly complementary, seem in fundamental disagreement only on the question of bending in poly(A) tracts. We believe that this disagreement must reflect erroneous assumptions in one or the other of these methods. The present study suggests that one of these is the assumption that MPD, and perhaps other dehydrating reagents as well, are neutral in their effects upon DNA structure of A-tracts. Thus, we believe that DNA structural models that are based upon crystallographic studies of oligonucleotides with A-tract-containing sequences must be taken with reservation, at least until structural data are available that address the solution conformation of A-tracts with a higher degree of certainty.

Acknowledgments— We thank Professor Ana Savic for reading the manuscript and Dr. Ivan Brukner for continuous discussions.

REFERENCES

1. Trifonov, E. N., and Sussman, J. L. (1980) *Proc. Natl. Acad. Sci. U. S. A.* **77,** 3816–3820
2. Marini, J. C., Levene, S. D., Crothers, D. M., and Englund, P. T. (1982) *Proc. Natl. Acad. Sci. U. S. A.* **79,** 7664–7668
3. Wu, H.-M., and Crothers, D. M. (1984) *Nature* **308,** 509–513
4. Hagerman, P. J. (1985) *Biochemistry* **24,** 7033–7044
5. Hagerman, P. J. (1986) *Nature* **321,** 449–450
6. Ulanovsky, L. E., and Trifonov, E. N. (1987) *Nature* **326,** 720–722
7. Ulanovsky, L., Bodner, M., Trifonov, E. N., and Choder, M. (1986) *Proc. Natl. Acad. Sci. U. S. A.* **83,** 862–866
8. Trifonov, E. N. (1985) *Crit. Rev. Biochem. Mol. Biol.* **19,** 89–106
9. Levene, S. D., and Crothers, D. M. (1983) *J. Biomol. Struct. Dyn.* **1,** 429–435
10. Koo, H.-S., Wu, H.-M., and Crothers, D. M. (1986) *Nature* **320,** 501–506
11. Koo, H.-S., and Crothers, D. M. (1988) *Proc. Natl. Acad. Sci. U. S. A.* **85,** 1763–1767
12. Satchwell, S., Drew, H. R., and Travers, A. A. (1986) *J. Mol. Biol.* **191,** 659–675
13. Milton, D. L., Casper, M. L., Wills, N. M., and Gesteland, R. F. (1990) *Nucleic Acids Res.* **18,** 817–820
14. McNamara, P. T., and Harrington, R. E. (1991) *J. Biol. Chem.* **266,** 12548–12554
15. Brukner, I., Dlakic, M., Savic, A., Susic, S., Pongor, S., and Suck, D. (1993) *Nucleic Acids Res.* **21,** 1025–1029
16. De Santis, P., Palleschi, A., Savino, M., and Scipioni, A. (1990) *Biochemistry* **29,** 9269–9273
17. Bolshoy, A., McNamara, P. T., Harrington, R. E., and Trifonov, E. N. (1991) *Proc. Natl. Acad. Sci. U. S. A.* **88,** 2312–2316
18. Crothers, D. M., Haran, T. E., and Nadeau, J. G. (1990) *J. Biol. Chem.* **265,** 7093–7096
19. Hagerman, P. J. (1990) *Annu. Rev. Biochem.* **59,** 755–781
20. Trifonov, E. N. (1991) *Trends Biochem. Sci.* **16,** 467–470
21. Haran, T. E., Kahn, J. D., and Crothers, D. M. (1994) *J. Mol. Biol.* **244,** 135–143
22. Nelson, H. C. M., Finch, J. T., Luisi, B. F., and Klug, A. (1987) *Nature* **330,** 221–226
23. Coll, M., Frederick, C. A., Wang, A. H.-J., and Rich, A. (1987) *Proc. Natl. Acad. Sci. U. S. A.* **84,** 8385–8389
24. Calladine, C. R., Drew, H. R., and McCall, M. J. (1988) *J. Mol. Biol.* **201,** 127–137
25. Maroun, R. C., and Olson, W. K. (1988) *Biopolymers* **27,** 585–603
26. DiGabriele, A. D., Sanderson, M. R., and Steitz, T. A. (1989) *Proc. Natl. Acad. Sci. U. S. A.* **86,** 1816–1820
27. Goodsell, D. S., Kopka, M. L., Cascio, D., and Dickerson, R. E. (1993) *Proc. Natl. Acad. Sci. U. S. A.* **90,** 2930–2934
28. Goodsell, D. S., Kaczor-Grzeskowiak, M., and Dickerson, R. E. (1994) *J. Mol. Biol.* **239,** 79–96
29. Goodsell, D. S., and Dickerson, R. E. (1994) *Nucleic Acids Res.* **22,** 5497–5503
30. Dlakic, M., and Harrington, R. E. (1995) *J. Biol. Chem.* **270,** 29945–29952
31. Harvey, S. C., Dlakic, M., Griffith, J., Harrington, R., Park, K., Sprous, D., and Zacharias, W. (1995) *J. Biomol. Struct. Dyn.* **13,** 301–307
32. Sprous, D., Zacharias, W., Wood, Z. A., and Harvey, S. C. (1995) *Nucleic Acids Res.* **23,** 1816–1821
33. Brukner, I., Susic, S., Dlakic, M., Savic, A., and Pongor, S. (1994) *J. Mol. Biol.* **236,** 26–32
34. Harrington, R. E. (1993) *Electrophoresis* **14,** 732–746
35. Drew, H. R., and Travers, A. A. (1984) *Cell* **37,** 491–502
36. Brukner, I., Jurukovski, V., and Savic, A. (1990) *Nucleic Acids Res.* **18,** 891–894
37. Tullius, T. D., and Dombroski, B. A. (1986) *Proc. Natl. Acad. Sci. U. S. A.* **83,** 5469–5473
38. McCarthy, J. G., Williams, L. D., and Rich, A. (1990) *Biochemistry* **29,** 6071–6081
39. Kitchin, P. A., Klein, V. A., Ryan, K. A., Gann, K. L., Rauch, C. A., Kang, D. S., Wells, R. D., and Englund, P. T. (1986) *J. Biol. Chem.* **261,** 11302–11309
40. Griffith, J., Bleyman, M., Rauch, C. A., Kitchin, P. A., and Englund, P. T. (1986) *Cell* **46,** 717–724
41. Wang, Y. H., Howard, M. T., and Griffith, J. D. (1991) *Biochemistry* **30,** 5443–5449
42. Griffith, J. D., and Christiansen, G. (1978) *Annu. Rev. Biophys. Bioeng.* **7,** 19–35
43. Dlakic, M., and Harrington, R. E. (1996) *Proc. Natl. Acad. Sci. U. S. A.* **93,** 3847–3852
44. Grzeskowiak, K., Goodsell, D. S., Kaczor-Grzeskowiak, M., Cascio, D., and Dickerson, R. E. (1993) *Biochemistry* **32,** 8923–8931
45. Travers, A. A. (1987) *Trends Biochem. Sci.* **12,** 108–112
46. Shrader, T. E., and Crothers, D. M. (1989) *Proc. Natl. Acad. Sci. U. S. A.* **86,** 7418–7422
47. Hogan, M. E., Roberson, M. W., and Austin, R. H. (1989) *Proc. Natl. Acad. Sci. U. S. A.* **86,** 9273–9277
48. Weston, S. A., Lahm, A., and Suck, D. (1992) *J. Mol. Biol.* **226,** 1237–1256
49. Brukner, I., Sanchez, R., Suck, D., and Pongor, S. (1995) *EMBO J.* **14,** 1812–1818
50. Borowiec, J. A., Zhang, L., Sasse-Dwight, S., and Gralla, J. D. (1987) *J. Mol. Biol.* **196,** 101–111
51. Sasse-Dwight, S., and Gralla, J. D. (1989) *J. Biol. Chem.* **264,** 8074–8081
52. Price, M. A., and Tullius, T. D. (1992) *Methods Enzymol.* **212,** 194–219
53. Tullius, T. D., and Dombroski, B. A. (1985) *Science* **230,** 679–681
54. Burkhoff, A. M., and Tullius, T. D. (1987) *Cell* **48,** 935–943
55. Zahn, K., and Blattner, F. R. (1987) *Science* **236,** 416–422
56. Crothers, D. M., Drak, J., Kahn, J. D., and Levene, S. D. (1992) *Methods Enzymol.* **212,** 3–29
57. Hagerman, P. J., and Ramadevi, V. A. (1990) *J. Mol. Biol.* **212,** 351–362
58. Koo, H.-S., Drak, J., Rice, J. A., and Crothers, D. M. (1990) *Biochemistry* **29,** 4227–4234
59. Livshits, M. A., and Lyubchenko, Y. L. (1994) *Mol. Biol.* **28,** 687–690
60. Shore, D., Langowski, J., and Baldwin, R. L. (1981) *Proc. Natl. Acad. Sci. U. S. A.* **78,** 4833–4837
61. Kahn, J. D., Yun, E., and Crothers, D. M. (1994) *Nature* **368,** 163–166
62. Marini, J. C., Effron, P. N., Goodman, T. C., Singleton, C. K., Wells, R. D., Wartell, R. M., and Englund, P. T. (1984) *J. Biol. Chem.* **259,** 8974–8979
63. Diekmann, S. (1987) *Nucleic Acids Res.* **15,** 247–265
64. Shore, D., and Baldwin, R. L. (1983) *J. Mol. Biol.* **170,** 957–981
65. Drew, H. R. (1984) *J. Mol. Biol.* **176,** 535–557
66. Suck, D., Lahm, A., and Oefner, C. (1988) *Nature* **332,** 464–468
67. Drew, H. R., and Travers, A. A. (1985) *J. Mol. Biol.* **186,** 773–790
68. Drew, H. R., and Calladine, C. R. (1987) *J. Mol. Biol.* **195,** 143–173
69. Herrera, J. E., and Chaires, J. B. (1989) *Biochemistry* **28,** 1993–2000
70. Lilley, D. M. J. (1992) *Methods Enzymol.* **212,** 133–139
71. Burkhoff, A. M., and Tullius, T. D. (1988) *Nature* **331,** 455–457
72. Price, M. A., and Tullius, T. D. (1993) *Biochemistry* **32,** 127–136
73. Buckin, V. A., Kankiya, B. I., Rentzeperis, D., and Marky, L. A. (1994) *J. Am. Chem. Soc.* **116,** 9423–9429
74. Dickerson, R. E., Goodsell, D., and Kopka, M. L. (1996) *J. Mol. Biol.* **256,** 108–125
75. Chan, S. S., Breslauer, K. J., Hogan, M. E., Kessler, D. J., Austin, R. H., Ojemann, J., Passner, J. M., and Wiles, N. C. (1990) *Biochemistry* **29,** 6161–6171

76. Chuprina, V. P. (1985) *FEBS Lett.* **186,** 98–102
77. Chuprina, V. P. (1987) *Nucleic Acids Res.* **15,** 293–311
78. Edwards, K. J., Brown, D. G., Spink, N., Skelly, J. V., and Neidle, S. (1992) *J. Mol. Biol.* **226,** 1161–1173
79. Kubinec, M. G., and Wemmer, D. E. (1992) *J. Am. Chem. Soc.* **114,** 8739–8740
80. Liepinsh, E., Otting, G., and Wuthrich, K. (1992) *Nucleic Acids Res.* **20,** 6549–6553
81. Quintana, J. R., Grzeskowiak, K., Yanagi, K., and Dickerson, R. E. (1992) *J. Mol. Biol.* **225,** 379–395
82. Buckin, V. A., Kankiya, B. I., Bulichov, N. V., Lebedev, A. V., Gukovsky, I. Y., Chuprina, V. P., Sarvazyan, A. P., and Williams, A. R. (1989) *Nature* **340,** 321–322
83. Buckin, V. A., Kankiya, B. I., Sarvazyan, A. P., and Uedaira, H. (1989) *Nucleic Acids Res.* **17,** 4189–4203
84. Marky, L. A., and Kupke, D. W. (1989) *Biochemistry* **28,** 9982–9988
85. Park, Y. W., and Breslauer, K. J. (1991) *Proc. Natl. Acad. Sci. U. S. A.* **88,** 1551–1555
86. Chan, S. S., Breslauer, K. J., Austin, R. H., and Hogan, M. E. (1993) *Biochemistry* **32,** 11776–11784
87. Olson, W. K., Marky, N. L., Jernigan, R. L., and Zhurkin, V. B. (1993) *J. Mol. Biol.* **232,** 530–554
88. Zhurkin, V. B., Ulyanov, N. B., Gorin, A. A., and Jernigan, R. L. (1991) *Proc. Natl. Acad. Sci. U. S. A.* **88,** 7046–7050
89. Schellman, J. A., and Harvey, S. C. (1995) *Biophys. Chem.* **55,** 95–114